This is the author-created version of the following work:

Guo, Zhifang, Wang, Jun, Deacon, Glen B., and Junk, Peter C. (2022) *Selective Oxidation of a Single Metal Site of Divalent Calix[4]pyrrolide Compounds [Ln2(N4Et8)(thf)4] (Ln = Sm or Eu), Giving Mixed Valent Lanthanoid(II/III) Complexes.* **Inorganic Chemistry, 61 (46) pp. 18678-18689.**

Access to this file is available from:

https://researchonline.jcu.edu.au/77142/

Please refer to the original source for the final version of this work:

https://doi.org/10.1021/acs.inorgchem.2c03172

Selective oxidation of a single metal site of divalent calix[4]pyrrolide compounds [Ln$_2$(N$_4$Et$_8$)(thf)$_4$] (Ln = Sm or Eu), giving mixed valent lanthanoid(II/III) complexes

Zhifang Guo, [a] Jun Wang, [a] Glen B. Deacon, [b] Peter C. Junk [a]*

[a]College of Science & Engineering, James Cook University, Townsville, QLD, 4811, Australia.

[b]School of Chemistry, Monash University, Clayton, VIC, 3800, Australia.

*Corresponding author: peter.junk@jcu.edu.au

Dedicated to *Professor Peter C. Junk* by his co-authors on the occasion of his 60th birthday

Abstract

The samarium(II) calix[4]pyrrolide complex [Sm$_2$(N$_4$Et$_8$)(thf)$_4$] (N$_4$Et$_8$ = *meso*-octaethylcalix[4]pyrrolide) undergoes selective oxidation of one Sm^{II} site on reaction with a range of metal carbonyls giving mixed valence Sm(II/III) complexes. Thus reactions with TM(CO)$_6$ (TM = Mo or Cr) entraps M$_2$(CO)$_{10}^{2-}$ ions between two mixed valence hosts in [{(thf)$_2$Sm^{II}(N$_4$Et$_8$)Sm^{III}(thf)(μ-OC)TM(CO)$_4$)}$_2$]·PhMe (TM = Mo, **1**; Cr, **2**), whilst W(CO)$_6$ on a different stoichiometry traps W(CO)$_5^{2-}$ in [{(thf)$_2$Sm^{II}(N$_4$Et$_8$)Sm^{III}(thf)}$_2${(μ-OC)W(CO)$_4$}]·PhMe **3** in which the isocarbonyl group is disordered over two sites. In contrast, [Sm$_2$(N$_4$Et$_8$)(thf)$_4$] reacts with dicobalt octacarbonyl, bis(cyclopentadienyl)tetracarbonyldiiron and dimanganese decacarbonyl to give the mixed valence species [(thf)$_2$Sm^{II}(N$_4$Et$_8$)Sm^{III}(thf)(μ-OC)TM(CO)$_3$)]·2PhMe (TM = Co, **4**; Fe, **5**), and [(thf)$_2$Sm^{II}(N$_4$Et$_8$)Sm^{III}(thf)(μ-OC)Mn(CO)$_4$)]·1.5PhMe **6**. However, both Sm^{II} sites of [Sm$_2$(N$_4$Et$_8$)(thf)$_4$] can be oxidized as its reaction with cyclooctatetraene (COT) yields the Sm^{III} species [(thf)Sm^{III}(N$_4$Et$_8$)Sm^{III}(COT)] **7**. The analogous Eu^{II} reagent, [Eu$_2$(N$_4$Et$_8$)(thf)$_4$] induces C-halogen activation of perfluorodecalin, hexachloroethane, and bromoethane to form the mixed oxidation state species [(thf)$_2$Eu^{II}(N$_4$Et$_8$)Eu^{III}(μ-X)]$_2$ (X = F, **8**; Cl, **9**; Br, **10**) despite the use of sufficient reagent to oxidize both Eu^{II} sites. The synthetic potential of the halogenido complexes was illustrated by reaction of **10** with sodium bis(trimethylsilyl)amide to give the mixed oxidation state [(thf)$_2$Eu^{II}(N$_4$Et$_8$)Eu^{III}(N(SiMe$_3$)$_2$)] **11**.

Introduction

Rare earth reductants based on samarium(II) and to lesser extent ytterbium(II) are noted for their capacity to trap unusual species by means of electron transfer reactions. The most widely used is bis(pentamethylcyclopentadienyl)samarium(II) (SmCp*$_2$), which has reduced dinitrogen, triphenylbismuth, triphenylantimony, carbon monoxide, elemental phosphorus, and more recently nanoscale Sb and arsenic to form the species N_2^{2-},[1] Bi_2^{2-},[2] Sb_3^{2-},[3] and $O_2C_3O^{2-}$,[4] P_8^{4-},[5] Sb_8^{4-}[6] and As_8^{4-},[7] respectively. Iron carbonyl sulfide clusters,[8] and arsenic sulfide species have also been reduced.[9] Iron and cobalt carbonyl anions have been incorporated by the less reducing YbCp*$_2$.[10] This behaviour is not restricted to pentamethylcyclopentadienyls, and the Sm and Yb derivatives of the bulky *N,N′*-bis(2,6-di-isopropylphenyl)formamidinate (DippForm) show analogous properties. Thus, [Sm(DippForm)$_2$(thf)$_2$] was used to trap [OC(Ph)=(C$_6$H$_5$)CPh$_2$O]$^{2-}$ (C$_6$H$_5$ = 1,4-cyclohexadiene-3-yl-6-ylidene), [SCSCS$_2$]$^{2-}$ and iron and cobalt carbonyl anions, by reactions with benzophenone and CS$_2$,[11] and metal carbonyls [12] respectively. [Ln(DippForm)$_2$(thf)$_2$] (Ln = Sm, Yb) complexes were also utilized to achieve polysulfide (3xS$_4^{2-}$),[13] and polypnictide (μ-η^4-Pn$_4$) (Pn = P, As) [14] incorporation and the Sm complex also trapped cyclopentadienylironpolypnictide moieties.[15] The less reactive [Yb(DippForm)$_2$(thf)] behaved differently from the Sm analogue with CS$_2$ and sandwiched the rare CS$_2^{2-}$ ion, and with sulfur the S$_3^{2-}$ ion.[16] The reactions with metal carbonyls also differed,[12] and the complex has also been used to trap a series of ketyl radical ion ligands.[17] Ln–TM carbonyl complexes have been widely studied, such as the single-molecule magnetic behaviour of Dy–TM carbonyl complexes,[18] and synthesis of Yb^{III}–TM [10] and Sm^{III}–Fe^0 [19] isocarbonyl complexes. Often, Ln^{II} complexes react with TM-carbonyls giving isocarbonyl-bridged systems with single-electron transfer (SET) to the TM carbonyl moiety. These species may then react further.[12] Ln^{II}–TM carbonyl complexes are also known.[20]

Meso-Octaethylcalix[4]pyrrole (H$_4$N$_4$Et$_8$) (Scheme 1) has received much attention in recent years owing to its flexible coordination behaviour and strong ability to stabilize many *d*-, *p*-, and *f*-block metal complexes,[21-28] including low-valent, mixed-valent and bimetallic complexes. The use of low-valent and mixed-valent lanthanoid calix[4]pyrrolide complexes is an attractive alternative in small molecule activation,[27] because of the high reducing ability and high Lewis acidity of the lanthanoids.
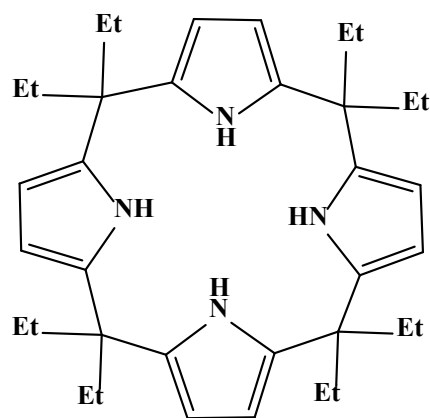
Scheme 1. *meso*-Octaethylcalix[4]pyrrole (H$_4$N$_4$Et$_8$)

Recently our group reported the first heteronuclear mixed-valent samarium(II/III)/ditungsten decacarbonyl calix[4]pyrrolide sandwich, [{(thf)$_2$Sm^{II}(N$_4$Et$_8$)Sm^{III}(thf)(OC)W(CO)$_4$)}$_2$]·2thf, with an unsupported W-W bond by the reduction of W(CO)$_6$ by a divalent samarium *meso*-octaethylcalix[4]pyrrolide.[26] In addition, a new mixed valent iodidoeuropium(II/III) calix[4]pyrrolide complex was also formed by the reaction of the analogous Eu^{II} complex with iodoethane,[26] It is the only such mixed valent Eu complex anchored by an N-donor ligand and is also the only one amongst the extremely rare organoeuropium(II/III) species showing a close Eu^{II}···Eu^{III} contact.

This paper reports the reduction of different TM carbonyls by the divalent samarium(II) calix[4]pyrrolide complex to give new heteronuclear mixed-valent samarium(II/III)/TM carbonyl complexes. Further, oxidation of the analogous Eu^{II} complex by different organic halides gives new mixed valent halidoeuropium(II/III) calix[4]pyrrolide complexes, which can be functionalised by sodium bis(trimethylsilyl)amide through metathesis, as an illustration of their synthetic potential.

Results and discussion

Synthesis of Mixed Valent Sm$^{II/III}$ Calix[4]pyrrolide complexes

Mixed oxidation state brown Sm$^{II/III}$ calix[4]pyrrolide sandwich complexes, [{(thf)$_2$Sm^{II}(N$_4$Et$_8$)Sm^{III}(thf)(μ-OC)TM(CO)$_4$)}$_2$]·PhMe (TM = Mo, **1**; Cr, **2**), and [{(thf)$_2$Sm^{II}(N$_4$Et$_8$)Sm^{III}(thf)}$_2${(μ-OC)W(CO)$_4$}]·PhMe **3** have been synthesized by the reactions of [Sm^{II}$_2$(N$_4$Et$_8$)(thf)$_4$] with molybdenum carbonyl, chromium carbonyl, and tungsten carbonyl respectively (Scheme 2 i, ii). The rare [TM$_2$(CO)$_{10}$]$^{2-}$ ions in compounds **1** and **2**, have unsupported Mo-Mo and Cr-Cr bonds within the mixed oxidation state sandwiches (Scheme 2 i). They are analogues of our previously reported [{(thf)$_2$Sm^{II}(N$_4$Et$_8$)Sm^{III}(thf)(μ-

OC)W(CO)$_4$)}$_2$]·2thf,[26] which has an encapsulated [W$_2$(CO)$_{10}$]$^{2-}$, apart from the difference in solvent of crystallization. The mixed valent complex [{(thf)$_2$Sm^{II}(N$_4$Et$_8$)Sm^{III}}$_2${(μ-OC)W(CO)$_4$}]·PhMe **3** was obtained by the reaction of [Sm$^{II}_2$(N$_4$Et$_8$)(thf)$_4$] and W(CO)$_6$ (mole ratio : 2:1; *cf.* 1:1 to trap W$_2$(CO)$_{10}{}^{2-}$ [26]). The two [Sm$^{II}_2$(N$_4$Et$_8$)(thf)$_4$] units are bridged by a 50% disordered μ-OC of [W(CO)$_5$]$^{2-}$ (Scheme 2 ii). On the other hand, [(thf)$_2$Sm^{II}(N$_4$Et$_8$)Sm^{III}(thf)(μ-OC)TM(CO)$_3$)]·2PhMe (TM = Co, **4**; Fe, **5**), and [(thf)$_2$Sm^{II}(N$_4$Et$_8$)Sm^{III}(thf)(μ-OC)Mn(CO)$_4$)]·1.5PhMe **6,** each with a single Sm-OC-TM bond, were synthesised from [Sm$^{II}_2$(N$_4$Et$_8$)(thf)$_4$] and dicobalt octacarbonyl, bis(cyclopentadienyl)tetracarbonyldiiron and dimanganese decacarbonyl, respectively (Scheme 2 iii, iv). For the compounds **1-6**, the dinuclear divalent [Sm$^{II}_2$(N$_4$Et$_8$)(thf)$_4$] has one Sm^{II} atom oxidized to Sm^{III} in the redox reactions and the other Sm^{II} atom remains in the divalent oxidation state. The Sm^{III} atom is bound to the isocarbonyl ligand in all cases, thereby giving a mixed-valent Sm^{II}Sm^{III} species. The two kinds of C-O bonds show intense stretching absorptions, at 1694 cm^{-1} (isocarbonyl) and 1898, 1987 cm^{-1} (terminal carbonyl) in the IR spectrum of complex **1**, and the assignments for all complexes are given in the Experimental Section and Table S1.

The formation of **1-3,** but not **4** and **6** is accompanied by elimination of CO, whilst formation of **5** requires elimination of ferrocene (Scheme 2). The trivalent [(thf)Sm^{III}(N$_4$Et$_8$)Sm^{III}(COT)] **7** complex was obtained by the reaction of [Sm$^{II}_2$(N$_4$Et$_8$)(thf)$_4$] and cyclooctatetraene (COT), and the cyan crystals formed immediately on adding COT to the [Sm$^{II}_2$(N$_4$Et$_8$)(thf)$_4$] solution (Scheme 2 v).

Good yields of crystalline products were obtained on deposition from the concentrated filtrates. Microanalyses of dried samples of bulk complexes **1-2** and **4-6**, **7** indicated loss of solvent of crystallization from the single crystal composition for **1-5** and, in the case of **1** and **2,** also loss of some coordinated thf. Compound **3** had a Sm analysis in accord with composition determined by X-ray crystallography.
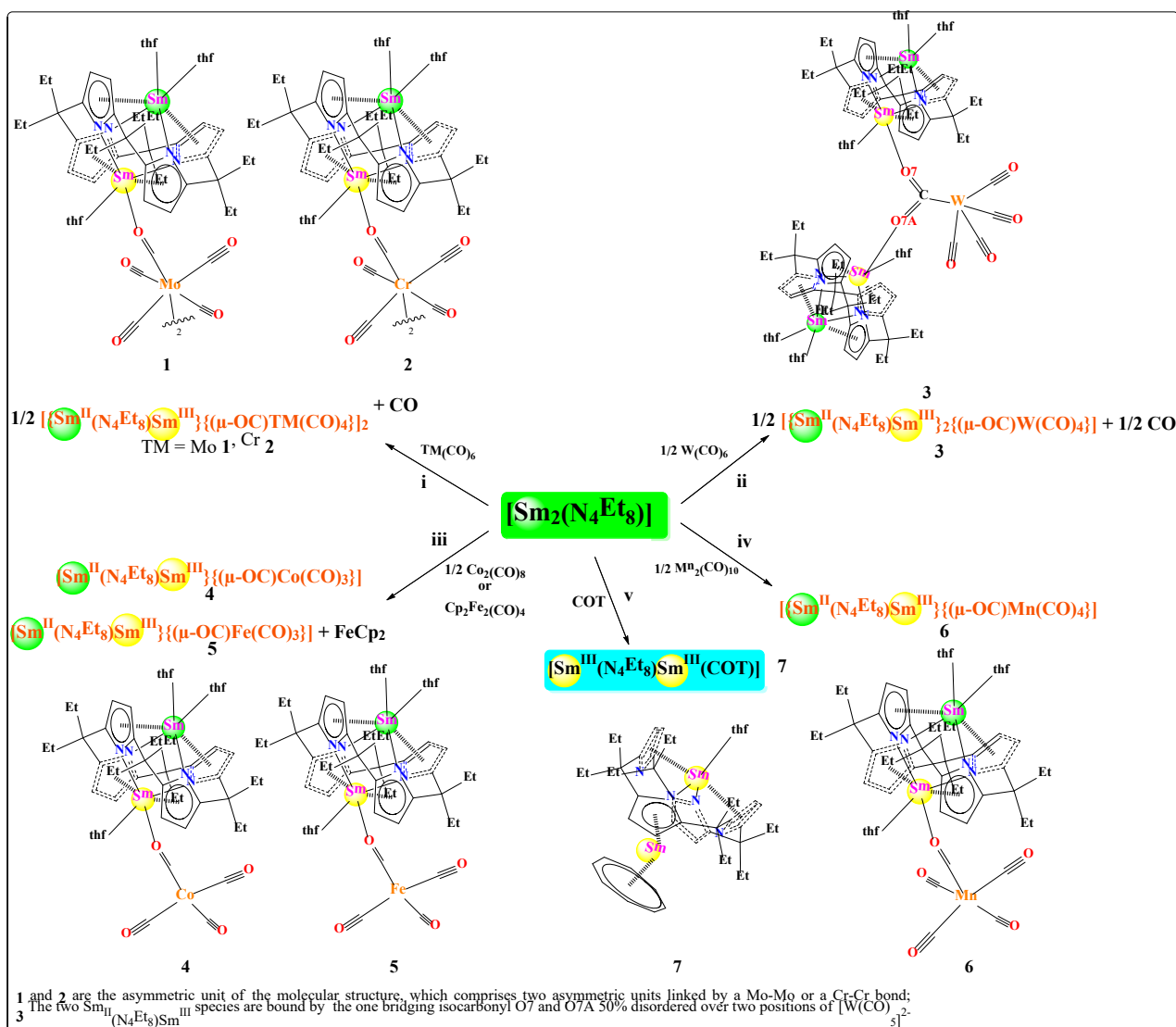
Scheme 2 Synthesis of compounds **1-7**

Structures of the complexes [{(thf)$_2$Sm^{II}(N$_4$Et$_8$)Sm^{III}(thf)}$_2${(μ-OC)$_2$TM$_2$(CO)$_8$}] [TM = Mo, 1; Cr, 2]

Single crystals of [{(thf)$_2$Sm^{II}(N$_4$Et$_8$)Sm^{III}(thf)(μ-OC)TM(CO)$_4$)}$_2$] [TM = Mo, 1; Cr, 2] are isomorphous and have unit cell parameters in agreement with those of [{(thf)$_2$Sm^{II}(N$_4$Et$_8$)Sm^{III}(thf)(μ-OC)W(CO)$_4$)}$_2$].[26] Complexes **1** and **2** crystallize in the monoclinic space group *C*2/*c* with one toluene molecule of crystallization. In the structure of **1** and **2** (Fig. 1), a [TM$_2$(CO)$_{10}$]$^{2-}$ ion is symmetrically positioned (two fold axis symmetry) between two Sm^{II}(N$_4$Et$_8$)Sm^{III} moieties. Complexes **1** and **2** are rare examples of structurally characterized complexes with a TM$_2$(CO)$_{10}$$^{2-}$ ion containing an unsupported TM-TM (Mo-Mo/Cr-Cr) bond according to the CCDC.[29] Both molybdenum atoms of **1** and chromium atoms of **2** are six-coordinate with four terminal carbonyl, one bridging isocarbonyl C-O between the TM (Mo/Cr) atom and Sm, and one TM-TM (Mo-Mo/Cr-Cr) bond. The isocarbonyl ligands

are κ^2-C,O bound, not κ^2-C,C, and the same is true for complexes **3-6** (below). The Mo-Mo bond length is 3.126(2)Å and the Cr-Cr bond length is 2.947(2) Å, similar to those reported: Mo-Mo [3.153 Å in $[C_{36}H_{30}NP_2]_2$ $[Mo_2(CO)_{10}]$ and 3.123 Å in $\{[(C_6H_5)P]_2\}_2[Mo_2(CO)_{10}]\cdot CH_2Cl_2$ and Cr-Cr [2.976 Å in $[2,2,2\text{-Crypt-Na}]_2$ $[Cr_2(CO)_{10}]$ and 2.974 Å in $\{[(C_6H_5)P]_2\}_2[Cr_2(CO)_{10}]\cdot CH_2Cl_2$.[30] The bridging isocarbonyl C-O bond (1.215(15) Å) between Sm and Mo atoms is longer than the average of the terminal carbonyl C-O bonds (1.14 Å). The bridging isocarbonyl C-O bond (1.195(9) Å) between Sm and Cr atoms is slightly longer than the average of the terminal carbonyl C-O bonds (1.16 Å). The Sm1-O1(isocarbonyl) bond [2.425(9), **1**; 2.427(5) Å, **2**] is significantly shorter than Sm1-O6(thf) [2.490(9), **1**; 2.506(5) Å, **2**]. The TM1-C1(isocarbonyl) bond length [1.888(13), **1**; 1.773(8) Å, **2**] is considerably shorter than the TM1-C(terminal carbonyl) bonds (2.00(2) to 2.05(2) Å, **1**; 1.830(15) to 1.884(11) Å, **2**). Similar behaviour has been observed in $[\{(thf)_2Sm^{II}(N_4Et_8)Sm^{III}(thf)(\mu\text{-OC})W(CO)_4\}_2]$.[26]

The cavity of each N_4Et_8 macrocycle is able to fit two metals in a 1,3-alternate arrangement. Thus, trivalent Sm1/Sm1# is coordinated in an η^5: κ^1: η^5: κ^1 manner wherein N1/N3 pyrrolide rings are η^5 bonded and N2/N4 atoms κ^1 bonded. Sm2/Sm2# are ligated by N_4Et_8 in a κ^1: η^5: κ^1: η^5 mode with κ^1 bonds from atoms N1/N3 and η^5 coordination of the N2/N4 pyrrolide rings. All Sm atoms are ten coordinate (η^5 bonded by the NC_4 pyrrolide being assigned to three coordination sites), regardless of oxidation state. The Sm2-N1/Sm2-N3 bond lengths (2.815(11)/2.826(10) Å in **1** and 2.850(6)/2.810(6) Å in **2**) are similar to the corresponding bond lengths of the Sm^{II} reagent, $[Sm^{II}_2(N_4Et_8)(thf)_4]$[25] (2.748(4) Å and 2.865(4) Å) and the Sm^{II}-N bond lengths of $[\{(thf)_2Sm^{II}(N_4Et_8)Sm^{III}(thf)(\mu\text{-OC})W(CO)_4\}_2]$ [2.842(7) Å and 2.804(7) Å].[26] They are much longer than Sm^{III}-N bond lengths [Sm1-N2/Sm1-N4: 2.584(9)/2.519(10) Å in **1** and 2.598(6)/2.526(5) in **2**], which are comparable to the analogous Sm^{III}-N values of $[\{(thf)_2Sm^{II}(N_4Et_8)Sm^{III}(thf)(\mu\text{-OC})W(CO)_4\}_2]$ [2.583(6)/2.511(6) Å].[26] Moreover, the Sm2-centroid (N2 ring) length (2.809 Å in **1** and in 2.805 **2**) and Sm2-centroid (N4 ring) (2.741 Å in **1** and **2**) are larger than Sm1-centroid (N1 ring) (2.573 Å in **1** and 2.570 Å in **2**) and Sm1-centroid (N3 ring) (2.536 Å in **1** and 2.552 Å in **2**) broadly consistent with the different sizes of Sm^{2+} and Sm^{3+}. The radii of Sm^{2+} is about 0.2 Å larger than the corresponding Sm^{3+} radius.[31] However, closer examination shows that the differences between comparable Sm^{II}-N (or centroid) and Sm^{III}-N (or centroid) distances are often greater (by 0.02–0.1 Å) than the expected *ca.* 0.2 Å for the same coordination number.[31] However this is compensated by the Sm-O(thf) bond length differences which are less than 0.1

Å, as also observed for $[\{(thf)_2Sm^{II}(N_4Et_8)Sm^{III}(thf)(\mu\text{-}OC)W(CO)_4\}_2]$.[26] As Sm^{III} has greater Lewis acidity than Sm^{II}, $[TM_2(CO)_{10}]^{2-}$ ions preferably bind to the former.
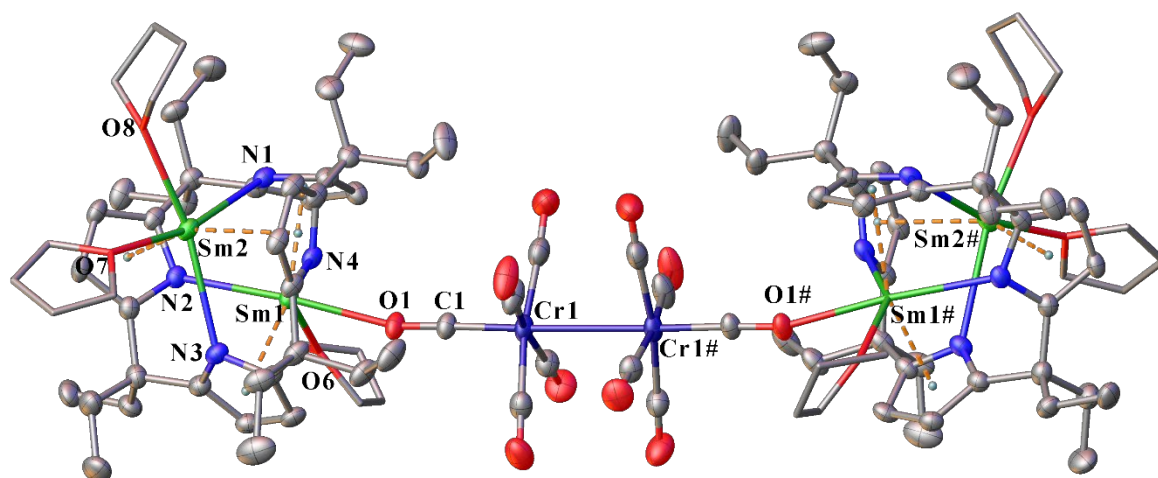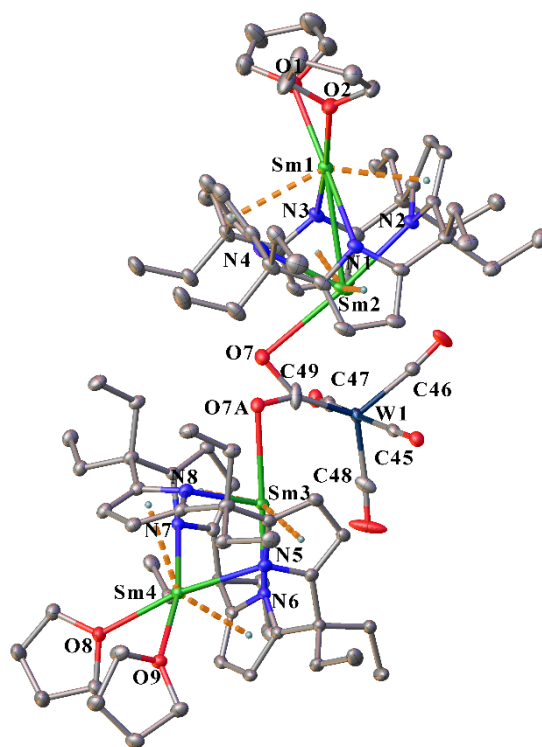

Figure 1. Molecular diagram of $[\{(thf)_2Sm^{II}(N_4Et_8)Sm^{III}(thf)(\mu\text{-}OC)Cr(CO)_4\}_2]$ (representative of Mo, **1**, Cr, **2**) represented by 50% thermal ellipsoids. The lattice PhMe molecules, disordered moiety and hydrogen atoms have been omitted and thf molecules were drawn as sticks for clarity. Selected bond angles (°) and lengths (Å): **1** Sm1-N2 2.584(9), Sm1-N4 2.519(10), Sm1-O1 2.425(9), Sm1-O6 2.490(9), Sm1-centroid (N1 ring) 2.573, Sm1-centroid (N3 ring) 2.536, Sm2-N1 2.815(11), Sm2-N3 2.826(10), Sm2-O7 2.574(8), Sm2-O8 2.559(8), Sm2-centroid (N2 ring) 2.809, Sm2-centroid (N4 ring) 2.741, O1-C1 1.215(15); Mo1-C1 1.888(13), Mo1-Mo1# 3.126(2), N2-Sm1-N4 110.8(3), N1-Sm2-N3 100.2(3), Centroid (N1 ring)-Sm1-centroid (N3 ring) 160.143, centroid (N2 ring)-Sm2-centroid (N4 ring) 143.695; **2** Sm1-N2 2.598(6), Sm1-N4 2.526(5), Sm1-O1 2.427(5), Sm1-O6 2.506(5), Sm1-centroid (N1 ring) 2.570, Sm1-centroid (N3 ring) 2.552, Sm2-N1 2.850(6), Sm2-N3 2.810(6), Sm2-O7 2.603(5), Sm2-O8 2.546(6), Sm2-centroid (N2 ring) 2.805, Sm2-centroid (N4 ring) 2.741, O1-C1 1.195(9); Cr1-C1 1.773(8), Cr1-Cr1# 2.947(2), N2-Sm1-N4 110.26(17), N1-Sm2-N3 100.26(17), centroid (N1 ring)-Sm1-centroid (N3 ring) 160.038, centroid (N2 ring)-Sm2-centroid (N4 ring) 143.858. Symmetry code: # = 1-X, +Y, 1/2-Z.

The complex $[\{(thf)_2Sm^{II}(N_4Et_8)Sm^{III}\}_2\{(\mu\text{-}OC)W(CO)_4\}]\cdot PhMe$ 3

Complex **3** crystallizes in the triclinic space group P-1 with one molecule of toluene in the lattice. A $[W(CO)_5]^{2-}$ ion is trapped by two mixed oxidation state $Sm^{II}(N_4Et_8)Sm^{III}$ cages (Fig. 2). A single isocarbonyl group disordered 50:50 over two positions binds the two $Sm_2(N_4Et_4)$ cages through trivalent Sm2/Sm3 atoms (Sm1/Sm4 are divalent). The tungsten atom is five coordinate with four terminal carbonyls and the one disordered bridging isocarbonyl C-O

7

between W and Sm2/Sm3. The bridging isocarbonyl C-O bond distances [O7-C49 1.414(11) and O7A-C49 1.273(10) Å] between Sm and W are longer than the average of the terminal carbonyl C-O bonds (1.157 Å). The W-C49(isocarbonyl) bond length [1.931(6) Å] is shorter than the W-C(terminal carbonyl) bonds [1.966(7) to 2.042(6) Å]. The two isocarbonyl ligands are angled at 61.09° to each other. The structure of **3** with a *cisoid* attachment of the cages differs from that of the reported structure of [{(thf)$_2$Sm^{II}(N$_4$Et$_8$)Sm^{III}(thf)(μ-OC)W(CO)$_4$)}$_2$] with *transoid* cages.[26] It is noteworthy that the –CO-Sm bond lengths (Sm2-O7 2.884(8) Å; Sm3-O7A 2.767(7) Å) are much longer than Sm-isocarbonyl bonding in **1-2** and **4-5** (e.g. **4** Sm1-O1 2.483(7) Å; **5** 2.508(5) Å). This is because the available electron density of a single carbonyl is shared over the two disordered carbonyl groups (C49-O7 and C49-O7A). Otherwise bond length relationships of the Sm$_2$(C$_4$H$_8$) cage are similar to those of complexes **1-2** and **4-5**.

Figure 2. Molecular diagram of **[{(thf)$_2$Sm^{II}(N$_4$Et$_8$)Sm^{III}}$_2${(μ-OC)W(CO)$_4$}]·PhMe** represented by 50% thermal ellipsoids, the two Sm^{II}(N$_4$Et$_8$)Sm^{III} species are bound by the one bridging isocarbonyl O7 and O7A 50% disordered over two positions of [W(CO)$_5$]$^{2-}$. The lattice PhMe molecule and hydrogen atoms have been omitted for clarity. Selected bond angles (°) and lengths (Å): Sm1-N1 2.800(5), Sm1-N3 2.772(5), Sm1-O1 2.572(5), Sm1-O2 2.558(5), Sm1-centroid (N2 ring) 2.822, Sm1-centroid (N4 ring) 2.789, Sm2-N2 2.556(4), Sm2-N4 2.557(6), Sm2-O7 2.884(8), Sm2-centroid (N1 ring) 2.561, Sm2-centroid (N3 ring) 2.589, O7-

C49 1.414(11), O7A-C49 1.273(10), W1-C49 1.931(6), N1-Sm1-N3 101.49(14), N2-Sm2-N4 109.88(16), centroid (N2 ring)-Sm1-centroid (N4 ring) 144.593, centroid (N1 ring)-Sm2-centroid (N3 ring) 159.075; Sm3-N6 2.547(4), Sm3-N8 2.544(5), Sm3-O7A 2.767(7), Sm3-centroid (N5 ring) 2.557, Sm3-centroid (N7 ring) 2.554, Sm4-N5 2.773(5), Sm4-N7 2.857(4), Sm4-O8 2.562(4), Sm4-O9 2.570(4), Sm4-centroid (N6 ring) 2.789, Sm4-centroid (N8 ring) 2.770, O7A-C49 1.273(10), N6-Sm3-N8 110.00(14), N5-Sm4-N7 100.58(13), centroid (N5 ring)-Sm3-centroid (N7 ring) 160.136, centroid (N6 ring)-Sm4-centroid (N8 ring) 143.936; W-C45 2.042(6), W-C46 1.980(6), W-C47 2.027(6), W-C48 1.966(7).

The complexes $[(thf)_2Sm^{II}(N_4Et_8)Sm^{III}(thf)(\mu\text{-}OC)TM(CO)_{3 \text{ or } 4})]$ [TM = Co, 4; Fe, 5; Mn, 6]

Complexes $[(thf)_2Sm^{II}(N_4Et_8)Sm^{III}(thf)(\mu\text{-}OC)Co(CO)_3]$ **4** and $[(thf)_2Sm^{II}(N_4Et_8)Sm^{III}(thf)(\mu\text{-}OC)Fe(CO)_3]$ **5** crystallize in the monoclinic space groups $P2_1/m$ and $P2_1/n$, respectively, and $[(thf)_2Sm^{II}(N_4Et_8)Sm^{III}(thf)(\mu\text{-}OC)Mn(CO)_4]$ **6** crystallizes in the triclinic space group P-1 (Fig. 3). The mixed oxidation state $Sm^{II}(N_4Et_8)Sm^{III}$ group is bound to the terminal $[TM(CO)_4]^-$ (TM = Co, **4**; Fe, **5**) or $[Mn(CO)_5]^-$ (**6**) ion by one bridging isocarbonyl C-O. Both the cobalt atom of **4** and the iron atom of **5** are four-coordinate with the three terminal carbonyl ligands and one bridging isocarbonyl C-O between Sm and the TM (Co/Fe) atom, and the manganese atom of **6** is five-coordinate with the four terminal carbonyl ligands and one bridging isocarbonyl C-O between Sm and the Mn atom. The bridging isocarbonyl C-O bond length [1.162(14), **4**; 1.171(11), **5**; 1.159(16) Å, **6**) between Sm and the TM atoms is similar to those in **1** and **2**. The TM1-C1(isocarbonyl) [1.702(12), **4**; 1.731(9), **5**; 1.778(15) Å, **6**] is slightly shorter than the average TM1-C(terminal carbonyl) bonds [1.73, **4**; 1.75, **5**; 1.82 Å, **6**]. Similar behaviour has been observed in complexes **1** and **2**.

Sm1 is bound by the macrocycle ligand in a η^5: κ^1: η^5: κ^1 manner (η^5 bonds from pyrrolide rings of N1/N1# for **4** and N1/N3 for **5** and **6**, and κ^1 bonds from N2/N3 for **4** and N2/N4 atoms for **5** and **6**) and Sm2 is bound by the macrocycle in a κ^1: η^5: κ^1: η^5 manner (κ^1 bonds of N1/N1# for **4** and N1/N3 atoms for **5** and **6**, and η^5 bonds from pyrrolide rings of N2/N3 for **4** and N2/N4 for **5** and **6**). Sm1 is trivalent and Sm2 is divalent. All Sm atoms are ten coordinate. The data for complex **6** were indicative of twinning leading to refinement issues, and therefore the crystal structure of **6** is reported for connectivity only and to establish proof of concept of synthetic utility. Bond lengths for **4-6** are given with Fig. 3, and the relationships derived therefrom are similar to those for **1** and **2**. Thus, Sm^{II}-N and Sm^{II}-centroid (N ring) distances

exceed Sm^{III}-N bond lengths and Sm^{II}-centroid (N ring) distances by ca 0.2 Å or more whereas the corresponding Sm-O bond lengths differ by less than 0.2 Å. Further, the Sm^{II}-N values are similar to those of the divalent reactant and both these and the Sm^{III}-N bond lengths correspond to those of **1**, **2**, and the reported [{(thf)$_2$Sm^{II}(N$_4$Et$_8$)Sm^{III}(thf)(μ-OC)W(CO)$_4$}$_2$.[26]
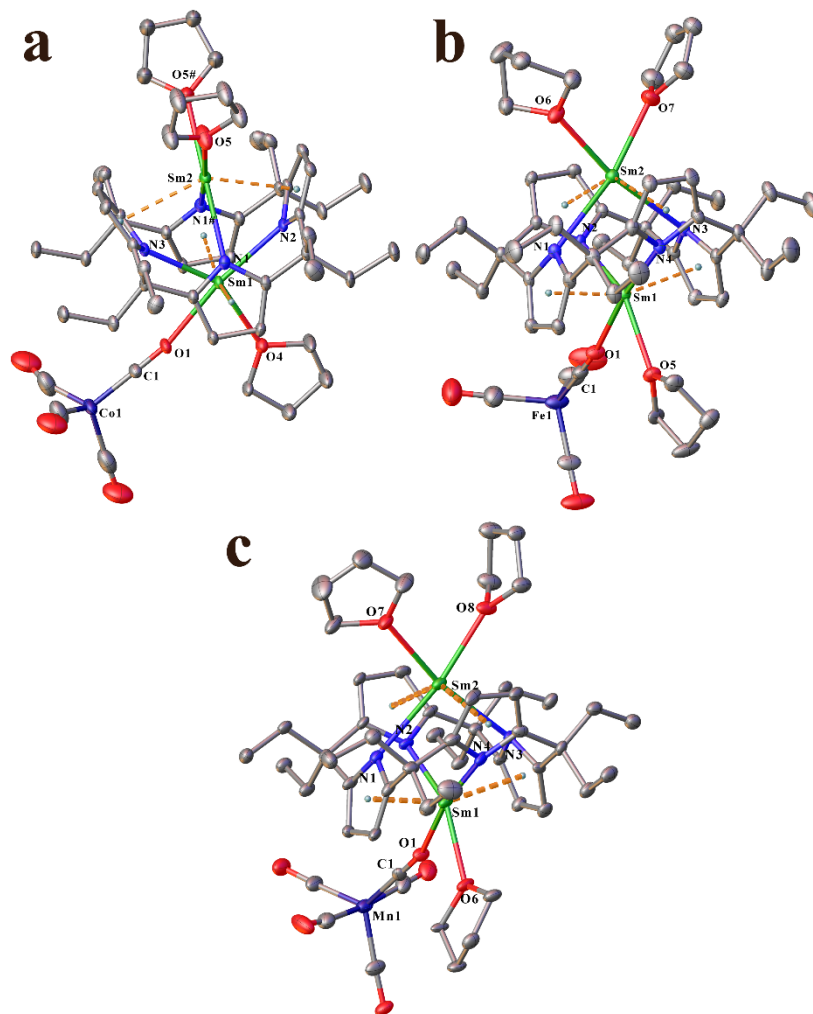
Figure 3. Molecular diagrams of **[(thf)$_2$Sm^{II}(N$_4$Et$_8$)Sm^{III}(thf)(μ-OC)TM(CO)$_3$)] (TM = Co, 4, Fig.3a; Fe, 5, Fig.3b**) and **[(thf)$_2$Sm^{II}(N$_4$Et$_8$)Sm^{III}(thf)(μ-OC)Mn(CO)$_4$)] 6, Fig.3c** represented by 50% thermal ellipsoids. The lattice PhMe molecules and hydrogen atoms have been omitted for clarity. Selected bond angles (°) and lengths (Å): **4** Sm1-N2 2.556(8), Sm1-N3 2.507(8), Sm1-O1 2.483(7), Sm1-O4 2.460(8), Sm1-centroid (N1 ring) 2.581, Sm2-N1 2.850(7), Sm2-O5 2.553(9), Sm2-centroid (N2 ring) 2.776, Sm2-centroid (N3 ring) 2.807, O1-C1 1.162(14); Co1-C1 1.702(12), N2-Sm1-N3 110.2(3), N1-Sm2-N1# 100.6(3), centroid (N1 ring)-Sm1-centroid (N1# ring) 160.633, centroid (N2 ring)-Sm2-centroid (N3 ring) 142.824, Symmetry code: # = 1+X, 1/2-Y, +Z. **5** Sm1-N2 2.508(6), Sm1-N4 2.564(6), Sm1-O1 2.508(5), Sm1-O5 2.470(6), Sm1-centroid (N1 ring) 2.565, Sm1-centroid (N3 ring) 2.567, Sm2-N1

2.841(7), Sm2-N3 2.858(7), Sm2-O6 2.564(7), Sm2-O7 2.561(7), Sm2-centroid (N2 ring) 2.841, Sm2-centroid (N4 ring) 2.805, O1-C1 1.171(11); Fe1-C1 1.731(9), N2-Sm1-N4 110.7(2), N1-Sm2-N3 99.93(19), centroid (N1 ring)-Sm1-centroid (N3 ring) 161.153, centroid (N2 ring)-Sm2-centroid (N4 ring) 142.624.

The complex [(thf)Sm^{III}(N$_4$Et$_8$)Sm^{III}(COT)] 7

[(thf)Sm^{III}(N$_4$Et$_8$)Sm^{III}(COT)] crystallizes in the monoclinic space group $P2_1/c$. Sm1 and Sm2 are trivalent in contrast to mixed oxidation state **1-6** . Sm1 is nine coordinate, bound by the N$_4$Et$_8$ macrocycle ligand in a η^5: κ^1: η^5: κ^1 manner (η^5 bonding by the N1/N3 pyrrolide rings and κ^1 bonds from N2/N4 atoms) and one thf ligand. Sm2 is eight coordinate, bound by the N$_4$Et$_8$ macrocycle ligand in a η^5 manner (by the N4 pyrrolide ring) and the (COT)$^{2-}$ ring in a η^8 manner (Fig. 4). The Sm1-N2/Sm1-N4 bond lengths (2.402(12)/2.549(11) Å) are comparable to analogous Sm^{III}-N values of **1** (2.519 (10), 2.584(9)). They are much shorter than Sm^{II}-N bond lengths of [Sm^{II}$_2$(N$_4$Et$_8$)(thf)$_4$] [25] [2.748(4) Å and 2.865(4) Å], consistent with the oxidation state assignments. Moreover, the Sm1-centroid (N1 ring) (2.502 Å) and Sm1-centroid (N3 ring) (2.469 Å), and Sm2-centroid (N4 ring) (2.524 Å), are comparable to analogous Sm^{III}-centroid (N ring) values of **1** (2.573 and 2.536 Å) but much shorter than those of Sm^{II}-centroid (N ring) (2.809 and 2.741 Å) of **1**, consistent with the Sm^{III} oxidation state. The Sm2-centroid (COT ring) distance is 1.865 Å, which is similar to the Sm^{III}-centroid (COT ring) value of eight coordinate (C$_5$Me$_5$)Sm(COT) (1.838 Å).[32] An open sandwich array is indicated by the centroid (N4 ring)-Sm2-centroid (COT ring) angle of (140.737°). Further supporting the assignment of the trivalent state to Sm1 is the reduction in coordination number compared to the starting material where there are two thf ligands bound to the Sm centre. Also, in all other complexes herein where there remains a divalent samarium centre, there are two thf ligands bound. The coordination number change from ten-coordinate for all divalent Sm atoms in this work and in the starting material compared with nine coordinate for Sm1 in compound **7** is in line with smaller ionic radii of Sm^{III} than Sm^{II}. [31]
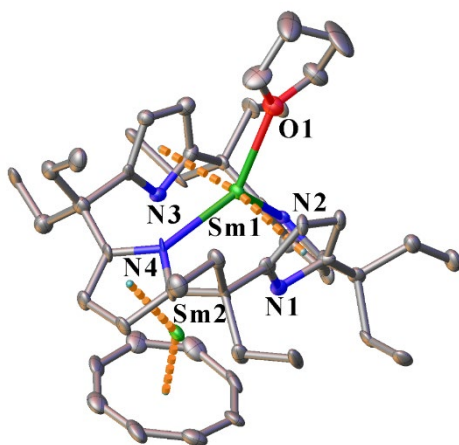
Figure 4. Molecular diagram of **[(thf)Sm^{III}(N$_4$Et$_8$)Sm^{III}(COT)]** (**7**) represented by 50% thermal ellipsoids. Hydrogen atoms have been omitted for clarity. Selected bond angles (°) and lengths (Å):): Sm1-N2 2.402(12), Sm1-N4 2.549(11), Sm1-O1 2.448(11), Sm1-centroid (N1 ring) 2.502, Sm1-centroid (N3 ring) 2.469, Sm2-centroid (N4 ring) 2.524, Sm2-centroid (COT ring) 1.865, N2-Sm1-N4 124.5(4), centroid (N1 ring)-Sm1-centroid (N3 ring) 168.797, centroid (N4 ring)-Sm2-centroid (COT ring) 140.737.

Synthesis of Mixed Valent Eu$^{II/III}$ Calix[4]pyrrolide complexes [(thf)$_2$Eu^{II}(N$_4$Et$_8$)Eu^{III}(μ-X)]$_2$ (X = F, 8; Cl, 9; Br, 10) and [(thf)$_2$Eu^{II}(N$_4$Et$_8$)Eu^{III}(N(SiMe$_3$)$_2$)] 11

The Eu^{II} complex [Eu$_2$(N$_4$Et$_8$)(thf)$_4$] was oxidized by perfluorodecalin, hexachloroethane, and bromoethane respectively, giving three new mixed-valent europium(II/III) calix[4]pyrrolide complexes [(thf)$_2$Eu^{II}(N$_4$Et$_8$)Eu^{III}(μ-X)]$_2$ (X = F, **8**; Cl, **9**; Br, **10**) in good yields (Scheme 3). The colour of the reaction mixture changed from reddish brown to dark green immediately after adding hexachloroethane. Hexachlorobutadiene showed similar reactivity, but oxidation by hexachlorobenzene was slower (see Experimental). For the synthesis of [(thf)$_2$Eu^{II}(N$_4$Et$_8$)Eu^{III}(μ-F)]$_2$, the reaction mixture was heated to 70 ˚C, and the colour changed to dark green after 30 min following addition of perfluorodecalin. To obtain [(thf)$_2$Eu^{II}(N$_4$Et$_8$)Eu^{III}(μ-Br)]$_2$, the reaction mixture was heated to 70 ˚C after addition of bromoethane and kept at this temperature for 24 h. Crystals suitable for X-ray crystallography were grown from thf in all cases. In compounds **8-10**, one Eu^{II} atom is oxidized to Eu^{III} whilst the other Eu^{II} atom is unaffected, thereby giving mixed-valent Eu^{II}Eu^{III} species. The synthetic potential of these halido complexes was illustrated by reaction of **10** with sodium bis(trimethylsilyl)amide giving [(thf)$_2$Eu^{II}(N$_4$Et$_8$)Eu^{III}(N(SiMe$_3$)$_2$)] **11** (Scheme 3). A similar complex [(thf)Eu^{II}(N$_4$Et$_8$)Eu^{III}(N(SiMe$_3$)$_2$)] was reported as arising from the reaction of [Eu(N(SiMe$_3$)$_2$)$_3$(μ-Cl)Li(thf)$_3$] with Et$_8$N$_4$H$_4$.[27] Complexes **8-11** gave microanalyses for the

bulk products as expected for the composition indicated by X-ray crystallography.
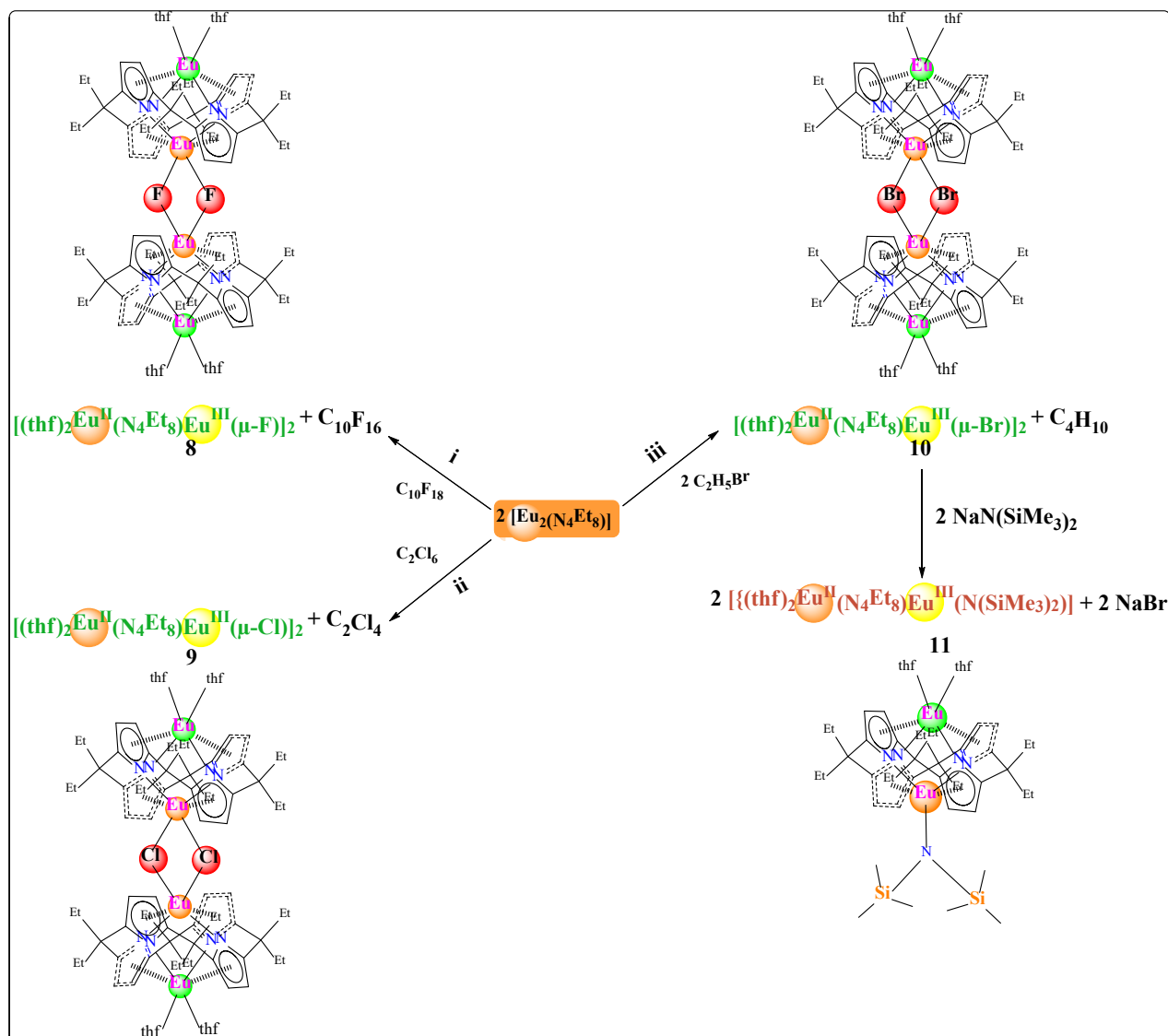
Scheme 3 Synthesis of compounds **8-11**

Structures of complexes [(thf)$_2$Eu^{II}(N$_4$Et$_8$)Eu^{III}(μ-X)]$_2$ (X = F, 8; Cl, 9; Br, 10)

[(thf)$_2$Eu^{II}(N$_4$Et$_8$)Eu^{III}(μ-F)]$_2$ (**8**) crystallizes in the monoclinic space group $P2_1/n$ with 1.5 molecules in the asymmetric unit with one dimer residing on an inversion centre, and [(thf)$_2$Eu^{II}(N$_4$Et$_8$)Eu^{III}(μ-Cl)]$_2$ (**9**) and [(thf)$_2$Eu^{II}(N$_4$Et$_8$)Eu^{III}(μ-Br)]$_2$ (**10**) (Fig. 5) crystallize in the $C2/m$ space group. In all structures, two mixed valent Eu^{II}(N$_4$Et$_8$)Eu^{III} cages are connected by two bridging halides (F, Cl, Br). Atoms Eu2/Eu4 for **10** and Eu2/Eu2* for **9** and **10** are divalent, and Eu1/Eu3 for **8** and Eu1/Eu1* for **9** and **10** are trivalent and all are ten coordinate. The coordination arrangement is similar to that of [(thf)$_2$Eu^{II}(N$_4$Et$_8$)Eu^{III}(μ-I)]$_2$.[26]

The Eu^{II}-N bond lengths [Eu2-N2, Eu2-N4, Eu4-N6, and Eu4-N8 for **8**, Eu2-N2 and Eu2-N3 for **9** and **10**, Fig. 5] are close to those of [Eu$^{II}_2$(N$_4$Et$_8$)(thf)$_4$] (2.762(7) Å).[26] They are longer than Eu^{III}-N [Eu1-N1, Eu1-N3, Eu3-N5, and Eu3-N7 of **8**, Eu1-N1 of **9** and **10**, Fig. 5], reflecting the different sizes of Eu^{2+} and Eu^{3+}. Similar differences are observed between the divalent Eu-centroid and the trivalent Eu-centroid distances (Fig. 5). The trivalent Eu atoms bind to two halide atoms forming a central four membered Eu$_2$(halide)$_2$ metallocycle. The average Eu-halide bond lengths, Eu-F 2.2828(4) Å for **8**, Eu1-Cl1 2.8058(11) Å for **9**, Eu1-Br1 2.9369(9) Å for **10**, are as expected, shorter than Eu-I (3.2349(16) and 3.2350(16) Å) in the ten coordinate [(thf)$_2$Eu^{II}(N$_4$Et$_8$)Eu^{III}(μ-I)]$_2$ complex,[26] in accord with halide ionic radii.[31] The Eu$^{II\cdots}$Eu^{III} distance [3.4069(6) of **8**, 3.4404(12) of **9**, 3.4343(12) Å for **10**], is similar to the Eu$^{II\cdots}$Eu^{III} distance 3.4163(6) of [(thf)$_2$Eu^{II}(N$_4$Et$_8$)Eu^{III}(μ-I)]$_2$,[26]
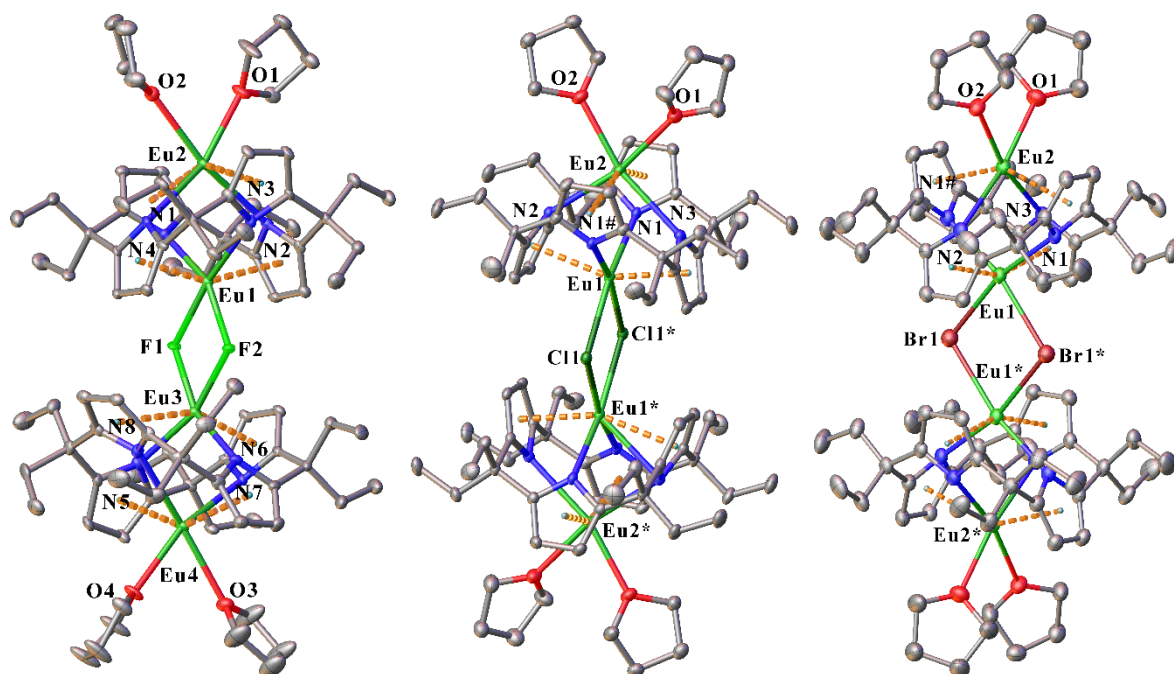
Figure 5. Molecular diagram of **[(thf)$_2$Eu^{II}(N$_4$Et$_8$)Eu^{III}(μ-F)]$_2$**, **[(thf)$_2$Eu^{II}(N$_4$Et$_8$)Eu^{III}(μ-Cl)]$_2$** and **[(thf)$_2$Eu^{II}(N$_4$Et$_8$)Eu^{III}(μ-Br)]$_2$** represented by 50% thermal ellipsoids. The lattice PhMe molecules and hydrogen atoms have been omitted for clarity. Selected bond angles (°) and lengths (Å): **8** Eu1-N1 2.574(6), Eu1-N3 2.655(6), Eu1-F1 2.333(4), Eu1-F2 2.263(4), Eu1-centroid (N2 ring) 2.663, Eu1-centroid (N3 ring) 2.577, Eu2-N2 2.799(6), Eu2-N4 2.745(6), Eu2-O1 2.545(5), Eu2-O2 2.596(6), Eu2-centroid (N1 ring) 2.790, Eu2-centroid (N4 ring) 2.805, N1-Eu1-N3 106.9(2), N2-Eu2-N4 103.50(17), centroid (N2 ring)-Eu1-centroid (N4 ring) 154.761, centroid (N1 ring)-Eu2-centroid (N3 ring) 146.321; Eu3-N5 2.565(6), Eu3-N7 2.591(6), Eu3-F1 2.250(4), Eu3-F2 2.285(4), Eu3-centroid (N6 ring) 2.542, Eu3-centroid

(N8 ring) 3.210, Eu4-N6 2.801(5), Eu4-N8 2.782(7), Eu4-O3 2.5620(6), Eu4-O4 2.546(5), Eu4-centroid (N5 ring) 2.808, Eu4-centroid (N7 ring) 2.807, N5-Eu3-N7 108.8(2), N6-Eu4-N8 98.91(18), centroid (N6 ring)-Eu3-centroid (N8 ring) 153.232, centroid (N5 ring)-Eu4-centroid (N7 ring) 144.655. **9** Eu1-N1 2.638(4), Eu1-Cl1 2.8058(11), Eu1-centroid (N2 ring) 2.612, Eu1-centroid (N3 ring) 2.603, Eu2-N2 2.770(5), Eu2-N3 2.761(5), Eu2-O1 2.592(6), Eu2-O2 2.566(5), Eu2-centroid (N1 ring) 2.752, N1-Eu1-N1# 107.27(16), N2-Eu2-N3 101.86(14), centroid (N2 ring)-Eu1-centroid (N3 ring) 154.840, centroid (N1 ring)-Eu2-centroid (N1# ring) 146.249. Symmetry code: * = 1-X,1-Y,-Z; # = +X,1-Y,+Z. **10** Eu1-N1 2.603(5), Eu1-Br1 2.9369(9), Eu1-centroid (N2 ring) 2.595, Eu1-centroid (N3 ring) 2.577, Eu2-N2 2.765(6), Eu2-N3 2.759(6), Eu2-O1 2.577(6), Eu2-O2 2.560(6), Eu2-centroid (N1 ring) 2.738, N1-Eu1-N1# 107.5(2), N2-Eu2-N3 101.27(18), centroid (N2 ring)-Eu1-centroid (N3 ring) 155.010, centroid (N1 ring)-Eu2-centroid (N1# ring) 146.086. Symmetry code: * = 1-X,1-Y,-Z; # = +X,1-Y,+Z.

Structure of $[(thf)_2Eu^{II}(N_4Et_8)Eu^{III}(N(SiMe_3)_2)]$ 11

$[(thf)_2Eu^{II}(N_4Et_8)Eu^{III}(N(SiMe_3)_2)$ **11** crystallizes in the monoclinic space group *Cc*. The N_4Et_8 macrocycle accommodates two Eu metal atoms in the cavity with a 1,3-alternate conformation. Eu1 atom is bound by the macrocycle in a $\eta^1:\eta^5:\eta^1:\eta^5$ manner (η^1 bonds from N1/N3 atoms and η^5 bonds from N2/N4 (pyrrolide rings) and the Eu2 atom is bound by the -N(macrocycle) ligand in a $\eta^5:\eta^1:\eta^5:\eta^1$ manner (η^5 bonds from N1/N3 pyrrolide rings and η^1 bonds from N2/N4) (Fig. 6). The trivalent Eu1 is nine-coordinate and bound to the bis(trimethylsilyl)amide group, while the divalent Eu2 atom is ten-coordinate and bound to two tetrahydrofuran molecules. The differences between the Eu^{II}-N and Eu^{III}-N bond lengths and between the Eu^{II}-centroid and Eu^{III}-centroid distances (Fig. 6) are much as expected from the foregoing Eu and Sm complexes. The Eu1-N5(silylamide) bond length [2.324(7) Å] is similar to that of $[(thf)Eu^{II}(N_4Et_8)Eu^{III}(N(SiMe_3)_2)]$ [2.306(4) Å].[27] The $Eu^{II}\cdots Eu^{III}$ distance [3.3837(10) Å] is slight shorter than the $Eu^{II}\cdots Eu^{III}$ distance in complexes **8-10** (above), and similar to the $Sm^{II}\cdots Sm^{III}$ distance in $[\{(thf)_2Sm^{II}(N_4Et_8)Sm^{III}(thf)(OC)W(CO)_4)\}_2]$ (3.3779(6) Å),[26] and the $Eu^{II}\cdots Eu^{III}$ distance [3.3626(6) Å] in $[(thf)Eu^{II}(N_4Et_8)Eu^{III}(N(SiMe_3)_2)]$.[27]
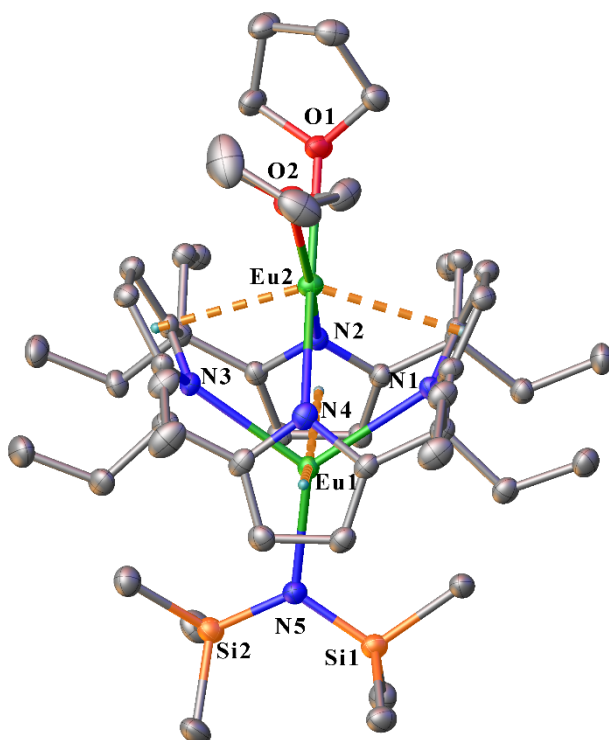
Figure 6. Molecular diagram of **[(thf)$_2$Eu^{II}(N$_4$Et$_8$)Eu^{III}(N(SiMe$_3$)$_2$)]** (**11**) represented by 30% thermal ellipsoids. Hydrogen atoms have been omitted for clarity. Selected bond angles (°) and lengths (Å): Eu1-N1 2.639(6), Eu1-N3 2.567(7), Eu1-N5 2.324(7), Eu1-centroid (N2 ring) 2.591, Eu1-centroid (N4 ring) 2.598, Eu2-N2 2.750(6), Eu2-N4 2.734(8), Eu2-O1 2.538(6), Eu2-O2 2.599(6), Eu2-centroid (N1 ring) 2.775, Eu2-centroid (N3 ring) 2.845, N1-Eu1-N3 108.9(2), N2-Eu2-N4 103.8(2), centroid (N2 ring)-Eu1-centroid (N4 ring) 155.459, centroid (N1 ring)-Eu2-centroid (N3 ring) 145.887.

Conclusions

The samarium(II) calix[4]pyrrolide complex [Sm^{II}$_2$(N$_4$Et$_8$)(thf)$_4$] reacts with TM(CO)$_6$ (TM = Mo, Cr, W) to trap TM$_2$(CO)$_{10}$$^{2-}$ (TM = Mo, Cr) or W(CO)$_5$$^{2-}$ sandwiched between [(thf)$_2$Sm^{II}(N$_4$Et$_8$)Sm^{III}(thf)] moieties, through two Sm^{III}–OC–TM linkages (**1**, **2**, **3**). On the other hand the samarium(II) reagent reduces Co$_2$(CO)$_8$, [FeCp(CO)$_2$]$_2$, and Mn(CO)$_5$ to give [(thf)$_2$Sm^{II}(N$_4$Et$_8$)Sm^{III}(thf)(OC)TM(CO)$_n$)] (TM = Co **4**, Fe **5**, n = 3; TM = Mn **6**, n = 4), and with COT, both Sm^{II} centres are oxidized giving [(thf)Sm^{III}$_2$ (N$_4$Et$_8$)(COT)] **7**.

The europium(II) analogue [Eu^{II}$_2$(N$_4$Et$_8$)(thf)$_4$] is able to initiate C-X (X = F, Cl, Br) activation of perfluorodecalin, hexachloroethane, and bromoethane to give [(thf)$_2$Eu^{II}(N$_4$Et$_8$)Eu^{III}(μ-X)]$_2$ (**8-10**) species in which only one europium(II) centre is oxidized even though sufficient oxidant was added to oxidize both. To illustrate the synthetic utility of the halogenido derivatives, the

bromido complex was treated with sodium bis(trimethylsilyl)amide to give [(thf)$_2$Eu^{II}(N$_4$Et$_8$)Eu^{III}(N(SiMe$_3$)$_2$)] **11**.

Experimental

General

The lanthanoid compounds described here are highly air- and moisture sensitive, hence were prepared and handled using vacuum-nitrogen line techniques and a dry box under an atmosphere of purified nitrogen. Lanthanoid metals were from Santoku/Molycorp/Eutectix. Large chunks were filed in the drybox before use. All other reagents were purchased from Sigma and used without purification. Solvents (thf, toluene, C$_6$D$_6$) were pre-dried by distillation over sodium or sodium benzophenone ketyl before being stored under an atmosphere of nitrogen over molecular sieves 3 Å. IR spectra were recorded as Nujol mulls between NaCl plates using a Perkin Elmer 1600 Series FTIR instrument within the range 4000–700 cm^{-1}. Proton decoupled ^{19}F NMR spectra were recorded with a Bruker 400MHz instrument. Microanalyses were determined by the Elemental Analysis Service, Macquarie University, and all the samples were sealed in tubes under nitrogen before transport. The metal analysis was carried out after decomposition of the sample with dilute HCl, buffering and complexometric titration with Na$_2$H$_2$(edta) and Xylenol Orange indicator. Crystals were immersed in crystallography oil and were examined on the MX1 beamline at the Australian Synchrotron. Sm$_2$(N$_4$Et$_8$) and Eu$_2$(N$_4$Et$_8$) were prepared by literature methods.[26, 28] Crystal data and refinement details are given in **Table S1**. CCDC 2204432-2204433 for compound **1-2**, 2204437 for compound **3**, 2204434-2204435 for compound **4-5**, 2204438-2204442 for compound **7-11**, contain the supplementary crystallographic data for this paper. These data can be obtained free of charge from The Cambridge Crystallographic Data Centre via www.ccdc.cam.ac.uk/data_request/cif.

Synthesis of [{(thf)$_2$Sm^{II}(N$_4$Et$_8$)Sm^{III}(thf)(OC)Mo(CO)$_4$)}$_2$]·PhMe 1

Molybdenum carbonyl (0.026 g, 0.10 mmol) in thf (0.50 mL) was added at ambient temperature to a green solution of [Sm$^{(II)}$$_2$(N$_4Et_8$)(thf)$_4$] (0.11 g, 0.10 mmol) in toluene (1.0 mL). The mixture was stored for three days, during which time, a brown crystalline solid precipitated. The solution was decanted and the residual solid was dried under vacuum (0.10 g, yield: 74%). IR (Nujol, cm^{-1}): 1987m, 1898s (terminal OC), 1694br.s (iso –OC), 1273m, 1242m, 1158w, 1039s, 978w, 923w, 890m, 825w, 792m, 762m, 730w. Elemental analysis calcd (%) for C$_{113}$H$_{152}$Mo$_2$N$_8$O$_{16}$Sm$_4$ (MW, 2671.70): C, 50.80; H, 5.73; N, 4.19;

$C_{90}H_{112}Mo_2N_8O_{12}Sm_4$ (MW, 2291.21, loss of PhMe of crystallization and four coordinated thf molecules): C, 47.18; H, 4.93; N, 4.89; found C, 47.16; H, 5.65; N, 4.85.

Synthesis of [{(thf)$_2$Sm^{II}(N$_4$Et$_8$)Sm^{III}(thf)(OC)Cr(CO)$_4$)}$_2$]·PhMe 2

Chromium carbonyl (0.022 g, 0.10 mmol) in thf (0.50 mL) was added at ambient temperature to a green solution of [Sm$^{(II)}_2$(N$_4$Et$_8$)(thf)$_4$] (0.11 g, 0.10 mmol) in toluene (1.0 mL). The mixture was stored for three days, during which time, a brown crystalline product precipitated. The solution was decanted and the solid remaining was dried under vacuum (0.08 g, 73%). IR (Nujol, cm^{-1}): 1968m, 1879s (terminal OC), 1716br.s (iso –OC), 1273w, 1241w, 1156w, 1038m, 984w, 927w, 889m, 827w, 791w, 762w, 729w. Elemental analysis calcd (%) for $C_{113}H_{152}Cr_2N_8O_{16}Sm_4$ (MW, 2583.82): C, 52.53; H, 5.93; N, 4.34; $C_{90}H_{112}Cr_2N_8O_{12}Sm_4$ (MW, 2203.33, loss of PhMe of crystallization and four coordinated thf molecules): C, 49.06; H, 5.12; N, 5.09; found C, 48.54; H, 5.96; N, 4.87.

Synthesis of [{(thf)$_2$Sm^{II}(N$_4$Et$_8$)Sm^{III}(thf)}$_2${(μ-OC)W(CO)$_4$}]·PhMe 3

Tungsten carbonyl (0.035 g, 0.10 mmol) in thf (0.50 mL) was added at ambient temperature to a green solution of [Sm$^{(II)}_2$(N$_4$Et$_8$)(thf)$_4$] (0.22 g, 0.20 mmol) in toluene (2.0 mL). The mixture was stored for 24 hours, during which time, brown crystalline product precipitated. The solution was decanted and the resulting crystals were dried under vacuum (0.18 g, yield: 76%), Anal. calcd (%) for $C_{100}H_{136}N_8O_9Sm_4W$ (2379.41): Sm 25.28. Found: Sm 25.16. IR (Nujol, cm^{-1}): 1982w, 1889s (terminal OC), 1701br.m (iso –OC), 1272w, 1241w, 1160w, 1039m, 978w, 926w, 889m, 830w, 788w, 762w, 728w.

Synthesis of [(thf)$_2$Sm^{II}(N$_4$Et$_8$)Sm^{III}(thf)(OC)Co(CO)$_3$)]·2PhMe 4

Dicobalt octacarbonyl (17 mg, 0.05 mmol) in thf (0.50 mL) was added at ambient temperature to a green solution of [Sm$^{(II)}_2$(N$_4$Et$_8$)(thf)$_4$] (0.11 g, 0.10 mmol) in toluene (1.0 mL). The mixture was stored for three days, during which time, brown crystals precipitated. The solution was decanted and the residual solid was dried under vacuum (0.11 g, yield: 78%). IR (Nujol, cm^{-1}): 2013m, 1913s, 1872w (terminal OC), 1795br.s (iso –OC), 1274m, 1242m, 1160m, 1030s, 978m, 926m, 870m, 836w, 787m, 764m, 731m. Elemental analysis calcd (%) for $C_{66}H_{88}CoN_4O_7Sm_2$ (MW, 1409.03): C, 56.26; H, 6.29; N, 3.98; $C_{52}H_{72}CoN_4O_7Sm_2$ (MW, 1224.80, loss of PhMe of crystallisation): C, 50.99; H, 5.92; N, 4.57; found C, 51.02; H, 6.04; N, 4.09.

Synthesis of [(thf)$_2$Sm^{II}(N$_4$Et$_8$)Sm^{III}(thf)(OC)Fe(CO)$_3$)]·2PhMe 5

Bis(cyclopentadienyl)tetracarbonyl-diiron (36 mg, 0.1 mmol) in thf (0.50 mL) was added at ambient temperature to a green solution of $[Sm^{(II)}_2(N_4Et_8)(thf)_4]$ (0.11 g, 0.10 mmol) in toluene (1.0 mL). The mixture was stored for three days, during which time, brown crystals precipitated. The solution was decanted and the solid remaining was dried under vacuum (0.12 g, yield: 85%). IR (Nujol, cm^{-1}): 1996m, 1954m, 1856m (terminal OC), 1784br.s (iso $-$OC), 1604s, 1261m, 1179w, 1071s, 1030s, 983w, 912m, 837w, 787m, 766m, 728s. Elemental analysis calcd (%) for $C_{66}H_{88}FeN_4O_7Sm_2$ (MW, 1405.95): C, 56.38; H, 6.31; N, 3.98; $C_{52}H_{72}FeN_4O_7Sm_2$ (MW, 1221.71, loss of PhMe of crystallisation) C, 51.12; H,5.94; N,4.57. found C, 51.15; H, 6.07; N, 4.59.

Synthesis of $[(thf)_2Sm^{II}(N_4Et_8)Sm^{III}(thf)(OC)Mn(CO)_4]\cdot1.5PhMe$ 6

Dimanganese decacarbonyl (19 mg, 0.05 mmol) in thf (0.50 mL) was added at ambient temperature to a green solution of $[Sm^{(II)}_2(N_4Et_8)(thf)_4]$ (0.11 g, 0.10 mmol) in toluene (1.0 mL). The mixture was stored for three days, during which time, brown crystals precipitated. The solution was decanted and the residual solid was dried under vacuum (0.10 g, yield: 71%). IR (Nujol, cm^{-1}): 2013m, 1917m, 1886s (terminal OC), 1769br.m (iso $-$OC), 1273m, 1240m, 1160w, 1037s, 1023s, 978m, 928m, 890m, 829w, 781m, 762m, 730w. Elemental analysis calcd (%) for $C_{63.5}H_{84}MnN_4O_8Sm_2$ (MW, 1386.98): C, 54.99; H, 6.10; N, 4.04; $C_{53}H_{72}MnN_4O_8Sm_2$ (MW, 1248.82, loss of 1.5 PhMe of crystallisation): C, 50.97; H, 5.81; N, 4.49; found C, 50.12; H,5.79; N, 4.60.

Synthesis of $[(thf)Sm^{III}(N_4Et_8)Sm^{III}(COT)]$ 7

Cyclooctatetraene (COT) (0.20 mmol) in thf (1 mL) was added at ambient temperature to a green solution of $[Sm^{(II)}_2(N_4Et_8)(thf)_4]$ (0.22 g, 0.20 mmol) in toluene (1.0 mL). The mixture colour changed to cyan immediately. The mixture was stored overnight, and the cyan crystals of $[(thf)Sm^{III}(N_4Et_8)Sm^{III}(COT)]$ precipitated. The solution was decanted and the crystals were dried under vacuum (0.15 g, yield: 75%). IR (Nujol, cm^{-1}): 1578w, 1323w, 1260m, 1153w, 1131w, 1045s, 1015s, 970m, 924s, 887m, 860m, 832m, 794s, 785s, 711s, 702s, 677w. Elemental analysis calcd (%) for $C_{48}H_{64}N_4OSm_2$ (MW, 1013.73): C, 56.87; H, 6.36; N, 5.53; found C, 56.76; H, 7.11; N, 6.01.

Synthesis of $[(thf)_2Eu^{II}(N_4Et_8)Eu^{III}(\mu-F)]_2$ 8

Toluene (2 mL) was added to a Schlenk flask charged with $[Eu_2(N_4Et_8)(thf)_4]$ (0.11 g, 0.1 mmol) and perfluorodecalin (0.09 g, 0.2 mmol). The mixture was heated to 70 ˚C, and the colour changed to dark green after 30 mins. During standing for 1 h, dark green powder,

[(Eu$_2$F(N$_4$Et$_8$)(thf)$_2$)$_2$], precipitated and was collected after decanting the solution (0.078 g, 78%). A small (0.3ml) aliquot of the solution was monitored by ^{19}F NMR. ^{19}F NMR (C$_6$D$_6$, 400 MHz, ppm): δ= -154, -162, which confirmed the consumption of C$_{10}$F$_{18}$ and formation of C$_{10}$F$_{16}$.[33] Crystals suitable for X-ray crystallography were grown from thf. IR (Nujol, cm^{-1}): 1327w, 1261s, 1222w, 1159w, 1095m, 1021br s, 955w, 926w, 889m, 818w, 796s, 765m, 724s, 700w, 660w. Elemental analysis calcd (%) for C$_{88}$H$_{128}$Eu$_4$F$_2$N$_8$O$_4$ (MW, 2007.82): C, 52.64; H, 6.43; N, 5.58; found C, 52.64; H, 6.51; N, 5.86.

Synthesis of [(thf)$_2$Eu^{II}(N$_4$Et$_8$)Eu^{III}(μ-Cl)]$_2$·1.5thf   9

Method 1: Toluene (5 mL) was added to a Schlenk flask charged with [Eu$_2$(N$_4$Et$_8$)(thf)$_4$] (0.11 g, 0.1 mmol) and hexachloroethane (0.03 g, 0.1 mmol). The mixture colour changed to dark green immediately. Overnight dark green crystalline [Eu$_2$Cl(N$_4$Et$_8$)(thf)$_2$]$_2$ precipitated and was collected after decanting the supernatant solution (0.090 g, 88%). IR (Nujol, cm^{-1}): 1326m, 1261s, 1235m, 1161w, 1095m, 1039 br s, 982 m, 927m, 893m, 827m, 787s, 769m, 728s, 694s, 680m. Crystals suitable for X-ray crystallography were grown from thf. Elemental analysis calcd (%) for C$_{94}$H$_{140}$Cl$_2$Eu$_4$N$_8$O$_{5.5}$ (MW, 2148.87): C, 52.54; H, 6.57; N, 5.21; found C, 51.70; H, 6.60; N, 5.95.

Method 2: Toluene (5 mL) was added to a Schlenk flask charged with [Eu$_2$(N$_4$Et$_8$)(thf)$_4$] (0.11 g, 0.1 mmol) and hexachlorobutadiene (0.03 g, 0.1 mmol). The mixture colour changed to dark green immediately. Overnight, dark green crystalline [Eu$_2$Cl(N$_4$Et$_8$)(thf)$_2$]$_2$ precipitated and was collected after decanting the solution (0.072 g, 71%). The identity was confirmed by a unit cell determination.

Method 3: Toluene (5 mL) was added to a Schlenk flask charged with [Eu$_2$(N$_4$Et$_8$)(thf)$_4$] (0.11 g, 0.1 mmol) and **hexachlorobenzene** (0.03 g, 0.1 mmol). The reaction was slower than method 1 and 2. The mixture was heated to 70 ˚C, and the colour changed to dark green after 2h, and overnight, dark green crystalline [Eu$_2$Cl(N$_4$Et$_8$)(thf)$_2$]$_2$ precipitated and was collected after decanting the solution (0.082 g, 80%). The identity was confirmed by a unit cell measurement.

Synthesis of [(thf)$_2$Eu^{II}(N$_4$Et$_8$)Eu^{III}(μ-Br)]$_2$·PhMe 10

Toluene (2 mL) was added to a Schlenk flask charged with [Eu$_2$(N$_4$Et$_8$)(thf)$_4$] (0.11 g, 0.1 mmol) and bromoethane (0.02 g, 0.2 mmol). The mixture was heated to 70 ˚C and kept at this temperature for 24 h and then stored at ambient temperature for two weeks, during which time dark green crystalline [Eu$_2$Br(N$_4$Et$_8$)(thf)$_2$]$_2$ precipitated and was then collected after decanting

the solution (0.084 g, 79%). IR (Nujol, cm^{-1}): 1323w, 1261s, 1223w, 1154w, 1095m, 1027 br s, 978w, 925w, 889m, 803m, 766m, 726s, 694w, 661w. Elemental analysis calcd (%) for $C_{95}H_{136}Br_2Eu_4N_8O_4$ (MW, 2221.77): C, 51.36; H, 6.17; N, 5.04; found C, 49.98; H, 6.24; N, 5.04.

Synthesis of [(thf)$_2$Eu^{II}(N$_4$Et$_8$)Eu^{III}(N(SiMe$_3$)$_2$)] 11

THF (2 mL) was added to a Schlenk flask charged with [Eu$_2$Br(N$_4$Et$_8$)(thf)$_2$]$_2$ (0.11 g, 0.05 mmol) and sodium bis(trimethylsilyl)amide (0.1 mmol). The mixture was stirred overnight and then stored at -20 °C for one day, when yellow crystalline [Eu$_2$(N(SiMe$_3$)$_2$)(N$_4$Et$_8$)(thf)$_2$] precipitated and was collected after decanting the solution (0.092 g, 80%). IR (Nujol, cm^{-1}): 1323m, 1261s, 1209w, 1177w, 1157m, 1072s, 1042s, 975m, 914s, 887s, 807s, 752s, 729s, 694m, 685m. Elemental analysis calcd (%) for $C_{50}H_{82}Eu_2N_5O_2Si_2$ (MW, 1145.30): C, 52.43; H, 7.22; N, 6.11; found C, 52.20; H, 7.06; N, 5.98.

Acknowledgements

Conflicts of Interest

There are no conflicts of interest to declare.

Associated Content

Supporting Information available: ^{19}F NMR spectra of reaction mixture for formation of complex **8**, terminal carbonyl and isocarbonyl stretching frequencies in IR spectra of complexes **1-6**, and X-ray crystallographic information, crystal data and structure refinement for complexes **1-11**.

References:

[1]. Evans, W. J.; Ulibarri, T. A.; Ziller, J. W. Isolation and x-ray crystal structure of the first dinitrogen complex of an f-element metal, $[(C_5Me_5)_2Sm]_2N_2$. *J. Am. Chem. Soc.* **1988**, *110*, 6877–6879.

[2]. Evans, W. J., Gonzales, S. L.; Ziller, J. W. Organosamarium-mediated synthesis of bismuth-bismuth bonds: x-ray crystal structure of the first dibismuth complex containing a planar $M_2(\mu-\eta^2:\eta^2-Bi_2)$ unit. *J. Am. Chem. Soc.* **1991**, *113*, 9880–9882.

[3]. Evans, W. J.; Gonzales, S. L.; Ziller, J. W. The utility of $(C_5Me_5)_2Sm$ in isolating crystallographically characterizable zintl ions. X-Ray crystal structure of a complex of $(Sb_3)^{3-}$. *Chem. Commun.* **1992**, 1138–1139.

[4]. Evans, W. J.; Grate, J. W.; Hughes, L. A.; Zhang, H.; Atwood, J. L. Reductive homologation of carbon monoxide to a ketenecarboxylate by a low-valent organolanthanide complex: synthesis and x-ray crystal structure of $[(C_5Me_5)_4Sm_2(O_2CCCO)(THF)]_2$. *J. Am. Chem. Soc.* **1985**, *107*, 3728–3730.

[5]. Konchenko, S. N.; Pushkarevsky, N. A.; Gamer, M. T.; Köppe, R.; Schnöckel, H.; Roesky, P. W. $[\{(\eta^5-C_5Me_5)_2Sm\}_4P_8]$: A Molecular Polyphosphide of the Rare-Earth Elements. *J. Am. Chem. Soc.* **2009**, *131*, 5740 –5741.

[6]. Schoo, C.; Bestgen, S.; Egeberg, A.; Klementyeva, S.; Feldmann, C.; Konchenko, S. N.; Roesky, P. W. Samarium polystibides derived from highly activated nanoscale antimony. *Angew. Chem., Int. Ed.* **2018**, *57*, 5912–5916.

[7]. Schoo, C.; Bestgen, S.; Egeberg, A.; Seibert, J.; Konchenko, S. N.; Feldmann, C.; Roesky, P. W. Samarium polyarsenides derived from nanoscale arsenic. *Angew. Chem., Int. Ed.*, **2019**, *58*, 4386–4389.

[8]. Konchenko, S. N.; Sanden, T.; Pushkarevsky, N. A.; Köppe, R.; Roesky, P. W. Wheel-shaped lanthanide iron sulfide clusters. *Chem. Eur. J.* **2010**, *16*, 14278–14280.

[9]. Arleth, N.; Bestgen, S.; Gamer, M. T.; Roesky, P. W. Realgar as a building block for lanthanide clusters: encapsulation of a copper cluster by a lanthanide cluster. *J. Am. Chem. Soc.* **2014**, *136*, 14023 –14026.

[10]. a) Tilley, T. D.; Andersen, R. A. Preparation and crystal structure of bis[bis(pentamethylcyclopentadienyl)ytterbium(III)] undecacarbonyltriferrate, $[(C_5Me_5)_2Yb]_2[Fe_3(CO)_{11}]$; a compound with four isocarbonyl (iron-carbonyl-ytterbium) interactions. *J. Am. Chem. Soc.* **1982**, *104*, 1772–1774; b) Tilley, T. D.; Andersen, R. A. Preparation and crystal structure of μ-carbonyl-OC-

bis(pentamethylcyclopentadienyl)(tetrahydrofuran)ytterbium(III)tricarbonylcobalt(I); A Yb–OC–Co linkage. *J. Chem. Soc. Chem. Commun*. **1981**, 985–986; c) Boncella, J. M.; Andersen, R. A. *J. Chem Soc. Chem. Commun*. **1984**, 809–810.

[11]. Deacon, G. B.; Junk, P. C.; Wang, J.; Werner, D. Reactivity of bulky formamidinatosamarium(II or III) complexes with C=O and C=S Bonds. *Inorg. Chem*. **2014**, *53*, 12553–12563.

[12]. Yadav, R.; Hossain, Md. E. Peedika Paramban, R.; Simler, T.; Schoo, C.; Deacon, G. B.; Junk, P. C.; Wang, J.; Roesky, P. 3d–4f heterometallic complexes by the reduction of transition metal carbonyls with bulky Ln^{II} amidinates. *Dalton Trans*. **2020**, *49*, 7701–7707.

[13]. Ma, Y.; Bestgen, S.; Gamer, M. T.; Konchenko, S. N.; Roesky, P. W. Polysulfide coordination clusters of the lanthanides. *Angew. Chem., Int. Ed*., **2017**, *56*, 13249–13252.

[14]. Schoo, C.; Bestgen, S.; Köppe, R.; Konchenko, S. N.; Roesky, P. W. Reactivity of bulky Ln(II) amidinates towards P_4, As_4, and As_4S_4. *Chem. Commun*., **2018**, *54*, 4770–4773.

[15]. Schoo, C.; Bestgen, S.; Schmidt, M.; Konchenko, S. N.; Scheer, M.; Roesky, P. W. Sterically induced reductive linkage of iron polypnictides with bulky lanthanide complexes by ring-opening of THF. *Chem. Commun*. **2016**, *52*, 13217–13220.

[16]. Werner, D.; Deacon, G. B.; Junk, P. C. Trapping CS_2^{2-} and S_3^{2-} between two ytterbium formamidinates. *Inorg. Chem*. **2019**, *58*, 1912–1918.

[17]. Werner, D.; Zhao, X.; Best, S. P.; Maron, L.; Junk, P. C.; Deacon, G. B. Bulky ytterbium formamidinates stabilise complexes with radical ligands, and related samarium "Tetracyclone" chemistry. *Chem. Eur. J.* **2017**, *23*, 2084–2102.

[18]. (a) Pugh, T.; Chilton, N. F.; Layfield, R. A. A Low-Symmetry dysprosium metallocene single-molecule magnet with a high anisotropy barrier. *Angew. Chem., Int. Ed*. **2016**, *55*, 11082–11085; (b) Burns, C. P.; Yang, X.; Wofford, J. D.; Bhuvanesh, N. S.; Hall, M. B.; Nippe, M. Structure and magnetization dynamics of Dy−Fe and Dy−Ru bonded complexes. *Angew. Chem., Int. Ed*. **2018**, *57*, 8144–8148.

[19]. Recknagel, A.; Steiner, A.; Brooker, S.; Stalke, D.; Edelmann, F. T. Organolanthanid(II)-Chemie: Synthese und Struktur von $[Cp_2Sm(-OC)_2FeCp]_2$. *Chem. Ber*. **1991**, *124*, 1373–1375.

[20]. (a) Evans, W. J.; Bloom, I.; Grate, J. W.; Hughes, L. A.; Hunter, W. E.; Atwood, J. L. Synthesis and characterization of the samarium-cobalt complexes $(C_5Me_5)_2(THF)SmCo(CO)_4$ and $[SmI_2(THF)_5][Co(CO)_4]$: x-ray crystal structure of a seven-coordinate samarium(III) cation complex. *Inorg. Chem*. **1985**, *24*, 4620–4623; (b) Beletskaya, I. P.;

Voskoboynikov, A. Z.; Chuklanova, E. B.; Kirillova, N. I.; Shestakova, A. K.; Parshina, I. N.; Gusev, A. I.; Magomedov, G. K. I. Bimetallic lanthanide complexes with lanthanide-transition metal bonds. Molecular structure of $(C_4H_8O)(C_5H_5)_2LuRu(CO)_2(C_5H_5)$. The use of ^{139}La NMR spectroscopy. *J. Am. Chem. Soc*. **1993**, *115*, 3156–3166; (c) Poplaukhin, P. V.; Chen, X.; Meyers, E. A.; Shore, S. G. Lanthanide−Transition metal carbonyl complexes: condensation of solvent-separated ion-pair compounds into extended structures. *Inorg. Chem*. **2006**, *45*, 10115–10125; (d) Oelkers, B.; Butovskii, M. V.; Kempe, R. f-Element–Metal bonding and the use of the bond polarity to build molecular intermetalloids. *Chem. Eur. J.* **2012**, *18*, 13566–13579; (e) Blake, M. P.; Kaltsoyannis, N.; Mountford, P. Probing the limits of alkaline earth–transition metal bonding: an experimental and computational study. *J. Am. Chem. Soc*. **2015**, *137*, 12352–12368.

[21]. a) Cuesta, L.; Sessler, J. L. π-Metal complexes of tetrapyrrolic systems. A novel coordination mode in "porphyrin-like" chemistry. *Chem. Soc. Rev*. **2009**, *38*, 2716–2729 and reference therein b) Jacoby, D.; Floriani, C.; Chiesi-Villa, A.; Rizzoli, C. Zirconium meso-octaethylporphyrinogen as a carrier for sodium hydride in toluene: zirconium-sodium bimetallic hydride and alkyls. *J. Am. Chem. Soc*. **1993**, *115*, 3595–3602; c) Jacoby, D.; Isoz, S.; Floriani, C.; Schenk, K.; Chiesi-Villa, A.; Rizzoli, C. Bifunctional carriers of organometallic functionalities: alkali-metal-zirconium-hydrido, -alkyl, and -allyl derivatives of meso-octaethylporphyrinogen and their reaction with isocyanides. *Organometallics*. **1995**, *14*, 4816-4824; d) Floriani, C.; Floriani-Moro, R. in The Porphyrin Handbook, Vol. 3 (Eds.: Kadish, K. M.; Smith, K. M.; Guilard, R.), Academic Press, San Diego, **2000**, pp. 385–402 and 405–420; e) Campazzi, E.; Solari, E.; Scopelliti, R.; Floriani, C. Lanthanide organometallic chemistry based on the porphyrinogen skeleton: acetylene and ethylene bridging praseodymium and neodymium η^5:η^1:η^5:η^1-bonded to meso-octaethylporphyrinogen. *Chem. Commun*. **1999**, 1617-1618; f) Bonomo, L.; Solari, E.; Martin, G.; Scopelliti, R.; Floriani, C. Porphyrinogen tetraanion functioning as a polymetallic assembler: nickel-meso-octaethylporphyrinogen binding four transition metal ions at the periphery. *Chem. Commun*. **1999**, 2319–2320; g) Franceschi, F.; Solari, E.; Scopelliti, R.; Floriani, C. Metal-mediated transfer of electrons between two different C−C single bonds that function as electron-donor and electron-acceptor units. *Angew. Chem. Int. Ed.* **2000**, *39*, 1685-1687; h) Floriani, C.; Solari, E.; Solari, G.; Chiesi-Villa, A.; Rizzoli, C. The π-pyrrole complexation of alkali metal ions by zirconium meso-octaalkylporphyrinogens: encapsulation of Li_4H_4 and Li_2O in

sandwich structures. *Angew. Chem. Int. Ed*. **1998**, *37*, 2245–2248; i) Solari, G.; Solari, E.; Floriani, C.; Chiesi-Villa, A.; Rizzoli, C. Bifunctional carriers of alkali-metal enolates: The use of zirconium meso-octaethylporphyrinogen in aldol condensation reactions. *Organometallics*. **1997**, *16*, 508–510; j) Bonomo, L.; Solari, E.; Scopelliti, R.; Floriani, C. The π complexation of alkali and alkaline earth ions by the use of meso-octaalkylporphyrinogen and aromatic hydrocarbons. *Chem. Eur. J.* **2001**, *7*, 1322–1332; k) Buranaprasertsuk, P.; Tangsakol, Y.; Chavasiri, W. Epoxidation of alkenes catalyzed by cobalt(II) calix[4]pyrrole. *Catal. Commun*. **2007**, *8*, 310–314; k) Sigmund, L. M.; Ehlert, C.; Enders, M.; Graf, J.; Gryn′ova, G.; Greb, L. Dioxygen activation and pyrrole α-cleavage with Calix[4]pyrrolato aluminates: enzyme model by structural constraint. *Angew. Chem. Int. Ed*. **2021**, *60*, 15632–15640; *Angew. Chem*. **2021**, *133*, 15761–15769.

[22]. a) Zhou, S.; Wang, H.; Ping, J.; Wang, S.; Zhang, L.; Zhu, X.; Wei, Y.; Wang, F.; Feng, Z.; Gu, X.; Yang, S.; Miao, H. Synthesis and characterization of organolanthanide complexes with a Calix[4]-pyrrolyl ligand and their catalytic activities toward hydrophosphonylation of aldehydes and unactivated ketones. *Organometallics*. **2012**, *31*, 1696–1702; b) Korobkov, I.; Gambarotta, S. Cis double addition of CO_2 to a coordinated arene of a thorium complex. *Organometallics*. **2004**, *23*, 5379–5381; c) Jubb, J.; Gambarotta, S. The surprising role of THF in vanadium macrocyclic chemistry. *Inorg. Chem*. **1994**, *33*, 2503–2504; d) Khorobkov, I.; Gambarotta, S.; Yap, G. P. A. A highly reactive uranium complex supported by the Calix[4]tetrapyrrole tetraanion affording dinitrogen cleavage, solvent deoxygenation, and polysilanol depolymerization. *Angew. Chem. Int. Ed*. **2002**, *41*, 3433–3436; e) Jubb, J.; Gambarotta, S.; Duchateau, R.; Teuben, J. H. Preparation and reactivity of the first yttrium porphyrinogen complex. *J. Chem. Soc., Chem. Commun*. **1994**, 2641–2642; f) Dube, T.; Gambarotta, S.; Yap, G. Samarium hydride, methyl, and vinyl complexes supported by Calix-tetrapyrrole ring macrocycle. thermal decomposition to samarium(II). *Organometallics*. **2000**, *19*, 121–126; g) Jubb, J.; Scoles, L.; Jenkins, H.; Gambarotta, S. Formation of bridging nitride versus terminal oxovanadium promoted by a vanadium(II) macrocyclic complex. *Chem. Eur. J.* **1996**, *2*, 767–771; h) Korobkov, I.; Gambarotta, S.; Yap, G. P. A. The first thorium arene complex: A divalent synthon. *Angew. Chem. Int. Ed*. **2003**, *42*, 814–818; i) Jubb, J.; Berno, P.; Hao, S.; Gamarotta, S. Nonsolvated Li-Amide Clusters. Preparation and crystal structure of the adduct {(meso-octaethylcalix-[4]-pyrrole)Li$_4$}(t-BuLi)$_2$ and of the tetrameric [(cyclohexyl)$_2$NLi]$_4$. *Inorg. Chem*. **1995**, *34*, 3563–3566; j) Dionne, M.; Jubb, J.; Jenkins,

H.; Wong, S.; Gambarotta, S. One- vs two-electron reduction of N_2O promoted by a divalent chromium macrocyclic complex. *Inorg. Chem*. **1996**, *35*, 1874–1879.

[23]. a) Ebner, F.; Greb, L. An isolable, crystalline complex of square-planar silicon(IV). *Chem*. **2021**, *7*, 2151–2159; b) Ruppert, H.; Sigmund, L. M.; Greb, L. Calix[4]pyrroles as ligands: recent progress with a focus on the emerging p-block element chemistry. *Chem. Commun*. **2021**, *57*, 11751–11763; c) Ruppert, H.; Greb, L. Calix[4]pyrrolato stannate(II): A tetraamido tin(II) dianion and strong metal-centered σ-donor. *Angew. Chem. Int. Ed*. **2022**, *61*, e202116615.

[24]. Song, J. I.; Gambarotta, S. The first dinuclear low-valent samarium complex with a short Sm–Sm contact. *Angew. Chem., Int. Ed. Engl*. **1995**, *34*, 2141–2143.

[25]. Dubé, T.; Gambarotta, S.; Yap, G. P. A. Dinuclear complexes of Di-, Tri-, and Mixed-Valent samarium supported by the Calix-tetrapyrrole ligand. *Organometallics*. **2000**, *19*, 817–823.

[26]. Deacon, G. B.; Guo, Z.; Junk, P. C.; Wang, J. Reductive trapping of $[(OC)_5W–W(CO)_5]^{2-}$ in a mixed-valent $Sm^{II/III}$ Calix[4]pyrrolide Sandwich. *Angew. Chem. Int. Ed*. **2017**, *56*, 8486–8489.

[27]. Mukthar, N. F. M.; Schley, N. D.; Ung, G. Alkali-metal- and halide-free dinuclear mixed-valent samarium and europium complexes. *Dalton Trans*. **2020**, *49*, 16059–16061.

[28]. Deacon, G. B.; Gardiner, M. G.; Junk, P. C.; Townley, J. P.; Wang, J. Rare-Earth metalation of Calix[4]pyrrole/Calix[4]arene free of alkali-Metal companions. *Organometallics*. **2012**, *31*, 3857–3864.

[29]. The survey was performed with CCDC: ConQuest 1.18, Version 5.37. For chromium there are four such examples with REFCODES: HIFFEH, KISMUU, PPNCRC, RERYUI; and for molybdenum there are three examples with REFCODES: JUKXUI, PPNMOC, QOVDAG.

[30]. (a) Handy, L. B.; Ruff, J. K.; Dahl, L. F. Structural characterization of the dinuclear metal carbonyl anions $[M_2(CO)_{10}]^{2-}$ (M = Cr, Mo) and $[Cr_2(CO)_{10}H]^-$. The Marked stereochemical effect of a linearly protonated metal-metal bond. *J. Am. Chem. Soc*. **1970**, *92*, 7312–7326; (b) Bachman, R. E.; Whitmire, K. H. Bis[bis(triphenylphosphine)iminium] decacarbonyldimolybdenum(Mo-Mo). *Acta Cryst*. **1993**, *C49*, 327–328; (c) Borrmann, H.; Pirani, A. M.; Schrobilgen, G. J. [2,2,2-Crypt-Na]$_2$[Cr$_2$(CO)$_{10}$]: A chromium(-1) carbonyl structure with a very weakly coordinating cation. *Acta Cryst*. **1997**, *C53*, 19–22.

[31]. Shannon, R. D. Revised effective ionic radii and systematic studies of interatomic distances in halides and chalcogenides. *Acta Crystallogr., Sect. A*, **1976**, *32*, 751–767.

[32]. Evans, W. J.; Johnston, M. A.; Clark, R. D.; Ziller, J. W. Variability of (ring centroid)-Ln-(ring centroid) angles in the mixed ligand C_5Me_5/C_8H_8 complexes $(C_5Me_5)Ln(C_8H_8)$ and $[(C_5Me_5)Yb(THF)](\mu-\eta^8:\eta^8-C_8H_8)[Yb(C_5Me_5)]$. *J. Chem. Soc., Dalton Trans*. **2000**, 1609–1612.

[33]. Robbins, A. J.; Ng, W. T. K.; Jochym, D.; Keal, T. W.; Clark, S. J.; Tozer, D. J.; Hodgkinson, P. Combining insights from solid-state NMR and first principles calculation: applications to the ^{19}F NMR of octafluoronaphthalene. *Phys. Chem. Chem. Phys*. **2007**, *9*, 2389–2396.

[34]. Cowieson, N. P.; Aragao, D.; Clift, M.; Ericsson, D. J.; Gee, C.; Harrop, S. J.; Mudie, N.; Panjikar, S.; Price, J. R.; Riboldi-Tunnicliffe, A.; Williamson, R.; Caradoc-Davies, T. MX1: a bending-magnet crystallography beamline serving both chemical and macromolecular crystallography communities at the Australian Synchrotron. *J. Synchrotron Radiat*. **2015**, *22*, 187–190.

GRAPHICAL ABSTRACT:

Selective oxidation of a single metal site of divalent calix[4]pyrrolide compounds [Ln$_2$(N$_4$Et$_8$)(thf)$_4$] (Ln = Sm or Eu), giving mixed valent lanthanoid(II/III) complexes

Zhifang Guo, Jun Wang, Glen B. Deacon, Peter C. Junk

Abstract

A number of rare heteronuclear mixed-valent samarium(II/III)/transition metal (TM) complexes were prepared by reactions of the divalent samarium(II) complex [Sm$_2$(N$_4$Et$_8$)(thf)$_4$] ((N$_4$Et$_8$)$_4$ = *meso*-octaethylcalix[4]pyrrolide) with transition metal carbonyls. Trivalent [(thf)Sm^{III}(N$_4$Et$_8$)Sm^{III}(COT)] complex was obtained by the reaction of [Sm$^{II}_2$(N$_4$Et$_8$)(thf)$_4$] with cyclooctatetraene (COT). The mixed-valent europium(II/III) complexes [(thf)$_2$Eu^{II}(N$_4$Et$_8$)Eu^{III}(μ-X)]$_2$ (X = F, Cl, Br) were prepared in good yield by oxidation of the Eu^{II} complex [Eu$_2$(N$_4$Et$_8$)(thf)$_4$] by halogen-alkanes.

M = Mo, Cr